Chitosan-based silver nanoparticles: A study of the antibacterial, antileishmanial and cytotoxic effects

Douglas dos Santos Lima[1,2], Beatriz Gullon[3,4], Alejandra Cardelle-Cobas[3], Lucas M Brito[1,2], Klinger AF Rodrigues[2], Patrick V Quelemes[1], Joilson Ramos-Jesus[1], Daniel DR Arcanjo[1,2], Alexandra Plácido[5], Krystallenia Batziou[6], Pedro Quaresma[6], Peter Eaton[6], Cristina Delerue-Matos[5], Fernando Aecio A Carvalho[2], Durcilene Alves da Silva[1], Manuela Pintado[3] and Jose Roberto de SA Leite[1,6,7]

Abstract

Silver nanoparticles have been studied as an alternative for treatment of microbial infections and leishmaniasis, without promoting induction of microbial or parasite resistance. In this study, chitosan-based silver nanoparticles were synthesized from silver nitrate ($AgNO_3$), sodium borohydride as a reducing agent, and the biopolymer chitosan as a capping agent. The chitosan-based silver nanoparticles were characterized by ultraviolet–visible, Fourier transform infrared, dynamic light scattering, zeta potential, atomic force microscopy, and transmission electron microscope. The antibacterial assay was performed by determination of the minimum inhibitory

[1]Research Center for Biodiversity and Biotechnology (BIOTEC), Federal University of Piauí (UFPI), Parnaíba, Brazil
[2]Medicinal Plants Research Center (NPPM), Federal University of Piauí (UFPI), Teresina, Brazil
[3]Center for Biotechnology and Fine Chemistry, Catholic University of Portugal, Porto, Portugal
[4]Department of Chemical Engineering, Institute of Technology, University of Santiago de Compostela, Santiago de Compostela, Spain
[5]REQUIMTE/LAQV, Polytechnic Institute of Porto (ISEP), Porto, Portugal
[6]UCIBIO/REQUIMTE, Department of Chemistry and Biochemistry, Faculty of Sciences, Porto University, Porto, Portugal
[7]Area of Morphology, Faculty of Medicine, University of Brasilia (UnB), Brasília, Brazil

Corresponding author:
Jose Roberto de SA Leite, Área de Morfologia, Faculdade de Medicina (FM), Universidade de Brasília (UnB), Campus Universitário Darcy Ribeiro, Asa Norte, Brasília 70910-900, Distrito Federal (DF), Brasil.
Email: jrsaleite@gmail.com; jrleite@pq.cnpq.br

concentration. The antileishmanial and the cytotoxic effects induced by AgNO$_3$, chitosan, and chitosan-based silver nanoparticles were analyzed by resazurin and MTT colorimetric assays, respectively. AgNO$_3$, chitosan, and chitosan-based silver nanoparticles induced a marked activity against all bacterial strains and promastigote forms of *Leishmania amazonensis* at minimum inhibitory concentrations ranging from 1.69 to 3.38 µg Ag/mL. Interestingly, the chitosan-based silver nanoparticles presented less cytotoxicity than the AgNO$_3$ alone and were more active against *L. amazonensis* than solely chitosan. Furthermore, the cytotoxic concentrations (CC$_{50}$) of both chitosan and chitosan-based silver nanoparticles against macrophages were significantly higher than the IC$_{50}$ against promastigotes. Thus, the chitosan-based silver nanoparticles represent a promising alternative for the treatment of microbial infections and leishmaniasis.

Introduction

Chitosan is a polysaccharide biopolymer derived from chitin, whose unique chemical structure forms a linear polycation with high charge density and reactive chemical groups, as well as excellent biocompatibility and manufacturing properties.[1] Therefore, the use of chitosan has been investigated for several technological and biomedical applications, such as pharmaceutical polymeric matrices for controlled drug release, due to its capability to dissolve non-water soluble drugs, and its long-lasting bioavailability, as well as its low toxicological, allergenic, and antimicrobial properties.[2,3]

A wide range of chemical groups are able to react with chitosan, such that chemical modifications can be used to either add specific functionalities or change biological or physical properties of the biopolymer.[4] In this sense, when structured at nanometric dimensions, silver possess different optical and biological properties which have been widely explored,[5] such as antibacterial and anticancer properties,[6] in the development of controlled drug release systems.[7] Currently, silver-induced biological properties are also under investigation for treatment of infected wounds and burns.[8,9] Likewise, the use of chitosan-based colloids has been reported for systemic release of several compounds and for synthesis of nanoparticles using metals, such as silver.[10,11]

The unique catalytic and surface characteristics of chitosan have a pivotal role in enhancing the antibacterial effect induced by silver nanoparticles.[10,11] The search for new antibacterial agents, especially with effects against resistant strains, represents a current global problem.[12] Furthermore, silver-doped metallic nanoparticles have also been studied against leishmaniasis,[13,14] a serious neglected disease with few and ever less effective options for chemotherapy treatment.[15] Therefore, this work focuses on the synthesis and characterization of chitosan-based silver nanoparticles (AgNPs-chitosan), and evaluates their effect against resistant bacteria and promastigote forms of *Leishmania amazonensis.*

Materials and methods

Synthesis and characterization of silver nanoparticles

The synthesis of Ag nanoparticles stabilized with chitosan was performed according to Wei et al.[10] with minor modifications. Silver nitrate (AgNO$_3$) and sodium borohydride (NaBH$_4$) were purchased from Aldrich Chemical Co. and used without further purification. Chitosan was purchased

from Sigma–Aldrich. The synthesis of AgNPs-chitosan was performed in a glass reactor with magnetic stirring. Briefly, 7 mL of 1 mM AgNO$_3$ solution was added to 7 mL of 0.05% chitosan solution (w/v), which was prepared by dissolving the chitosan in 1% aqueous acetic acid. To reduce the silver salt, a measured amount of fresh NaBH$_4$ stock solution (0.1 M) was added to the AgNO$_3$ solution containing chitosan as a capping agent. This solution acquired a yellow-gray turbid aspect after the addition of NaBH$_4$, and then a colloidal suspension was formed.

The synthesis of silver nanoparticles was monitored by ultraviolet–visible (UV–vis)-near-infrared spectroscopy (NIR) scanning spectrophotometer (UV-3101 PC; Shimadzu, Japan) at the range of 300–800 nm. Particle size and zeta potential (ζ) measurements were carried out using a Malvern Zetasizer Nano, Model ZS 3600. The hydrodynamic diameter was measured by dynamic light scattering (DLS) at wavelength of 633 nm and fixed scattering angle of 173°. Particle size was measured considering the particle as spherical shape. Each sample was measured three times for two replicate samples at a constant temperature of 25°C ± 1°C. All infrared measurements were performed on a Fourier transform infrared (FTIR) spectrophotometer (FT-IR System *Spectrum BX*; PerkinElmer) using the attenuated total reflection (ATR) technique in the spectral range from 4000 to 650 cm^{-1}.

To quantify the percentage of silver in solution, the atomic absorption spectroscopy (Varian—Model AA240FS) was used, with a wavelength of 328.1 nm and multielement lamp (Varian no. 5610108700). The reading was held in atomic absorption flame with oxygen and acetylene gases. Samples for transmission electron microscope (TEM) analysis were prepared by depositing 10 µL of the colloidal suspensions on carbon copper grids, washing twice with 10 mL of Milli-Q water, followed by air-drying. TEM was performed by a Hitachi H-8100 microscope operating at 200 kV. Histograms of the nanoparticle size distribution were generated with ImageJ®, a freely available image analysis program (http://rsb.info.nih.gov/ij/) and Origin 9.0®. Atomic force microscopy (AFM) samples were prepared by drying a drop of nanoparticle solution onto a freshly cleaved mica surface. Samples were analyzed by an AFMWorkshop TT-AFM (Signal Hill, USA) on vibrating mode, using a scanner of 15 × 15 × 7 µm. AppNano ACT probes were used at an oscillation frequency close to 300 kHz, and the images were analyzed using the Gwyddion® 2.42 package.

Biological assays

Antibacterial evaluation. To evaluate the antibacterial effect of AgNPs-chitosan, the following microorganisms were used: Gram-positive methicillin-resistant *Staphylococcus aureus* (MRSA) ATCC 43300 and the Gram-negative organisms extended-spectrum beta-lactamases (ESBL) *Escherichia coli* ATCC 35218 and *Klebsiella pneumoniae* ATCC 700603. The microorganisms were cultured under aerobic conditions in Mueller–Hinton agar at 37°C for 24 h. Afterward, a suspension of bacterial strains was prepared in 0.85% NaCl solution, with an optical density of 0.5 McFarland (1×10^8 colony-forming unit (CFU)/mL), and then used as the inoculum in the experiment.

The antibacterial assay was performed by determination of the minimum inhibitory concentration (MIC) of AgNPs-chitosan, following the method of Quelemes et al.[16] The strains (concentration of 5×10^5 CFU/mL) were exposed to twofold dilution series of the AgNPs-chitosan (0.42–27 µg Ag/mL) in a 96-well microdilution plate. The MICs of chitosan, AgNO$_3$, and standard antibiotics effective against the bacteria were also determined. At the end of the microdilution, the tested concentrations ranged from 0.42 to 27 µg Ag/mL for AgNO$_3$, 1.95 to 125 µg/mL for chitosan, and 0.5 to 16 µg/mL for antibiotics. The MIC was defined as the lowest concentration of agent which is able to restrict the visible bacterial growth in the culture media. All assays were performed in triplicate.

Antileishmanial evaluation against promastigote forms of L. amazonensis. *Leishmania amazonensis* (IFLA/BR/67/PH8) was maintained as amastigotes over several weekly passages in Swiss mice and in vitro as promastigotes at 26°C in supplemented Schneider's medium, pH 7.0 (10% heat-inactivated fetal bovine serum (FBS), 100 U/mL penicillin, and 100 μg/mL streptomycin), as previously described.[17] The inhibition of parasite growth was assayed using the resazurin (alamarBlue®) colorimetric assay.[18,19] Briefly, promastigotes in the logarithmic growth phase were cultured in 96-well cell culture plates at 1×10^6 parasites per well in 100 μL of Schneider's medium with increasing concentrations of AgNPs-chitosan, chitosan, and AgNO$_3$. These agents were prepared at a twofold dilution series, with concentrations ranging from 0.42 to 27 μg Ag/mL for AgNPs-chitosan, 1.95 to 125 μg/mL for chitosan, and 0.42 to 27 μg Ag/mL for AgNO$_3$. The plates were incubated for 48 h in a biological oxygen demand (BOD) incubator at 26°C. Cell viability was measured by adding 20 μL of resazurin (1 mM) followed by incubation for 6 h in BOD at 26°C. The absorbance was measured using an ELISA plate reader (Biosystems model ELx800) at 550 nm. Schneider's medium in the presence of 1×10^6 of *Leishmania* was used as a negative control, being considered as 100% of the parasite viability.

Cytotoxic effect and determination of the selective index. Male and female BALB/c mice (4–5 weeks old) were maintained under controlled temperature (24°C±1°C) and light conditions (12-h light–dark cycle). Murine peritoneal macrophages were collected 5 days after intraperitoneal administration of 3% thioglycollate (1.5 mL). The protocols were approved by the Animal Experimentation Ethics Committee from Federal University of Piauí, permission no. 008/12) and were carried out according to the current guidelines for the care of laboratory animals and the ethical guidelines for investigation of experimental pain in conscious animals (NIH publication 85-23, revised in 1985).

Cytotoxicity evaluation was carried out in 96-well plates using the MTT assay. Approximately 1×10^6 macrophages per well were incubated in 100 μL of supplemented RPMI 1640 medium at 37°C and 5% CO$_2$ for 4 h for cell adhesion. Non-adherent cells were removed by washing with RPMI 1640 medium. Then, AgNPs-chitosan, AgNO$_3$, and chitosan solutions were diluted in supplemented RPMI 1640 medium for testing cell viability at a two-fold dilution series, at concentrations ranging from 0.42 to 27 μg Ag/mL for AgNPs-chitosan, 1.95 to 125 μg/mL for chitosan, and 0.42 to 27 μg Ag/mL for AgNO$_3$. The plates were incubated at 37°C with 5% CO$_2$ for 2 days. Following incubation, cytotoxicity was assessed by adding 10 μL of MTT (5 mg/mL) for 4 h. The supernatant was discarded, and the formazan crystals were dissolved by addition of 100 μL of dimethyl sulfoxide (DMSO). Finally, the absorbance was measured at 550 nm using a microplate reader.

The selectivity index (SI) of each treatment was calculated by the ratio between the mean cytotoxicity concentration (CC$_{50}$) against murine macrophages and the mean inhibitory concentration (IC$_{50}$) of promastigotes' growth.

Antileishmanial evaluation against amastigote forms of L. amazonensis. The peritoneal macrophages were isolated from the peritoneum of BALB/c mice by injecting the cold phosphate-buffered saline (PBS) and re-aspiration. Isolated macrophages were seeded on a glass coverslip in tissue culture 12-well plates and incubated at 37°C with 5% CO$_2$ for 24 h. Non-adherent cells were removed by two washes with PBS. Adherent macrophages were infected with the stationary growth phase of promastigote forms of *L. amazonensis* at a parasite–macrophage ratio of 10:1 and then the plate was incubated for 24 h at 37°C with 5% CO$_2$. Non-internalized promastigotes were removed by washing with cold PBS. Infected macrophages were further incubated in the presence or absence (negative control group) of concentrations of the AgNPs-chitosan and controls for 24 and 48 h. Infected macrophages in coverslip were stained with Giemsa stain, and the amastigotes inside the macrophage (100 macrophages per coverslip) were counted under a light microscope.[20]
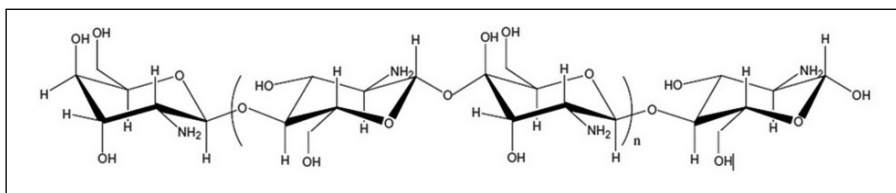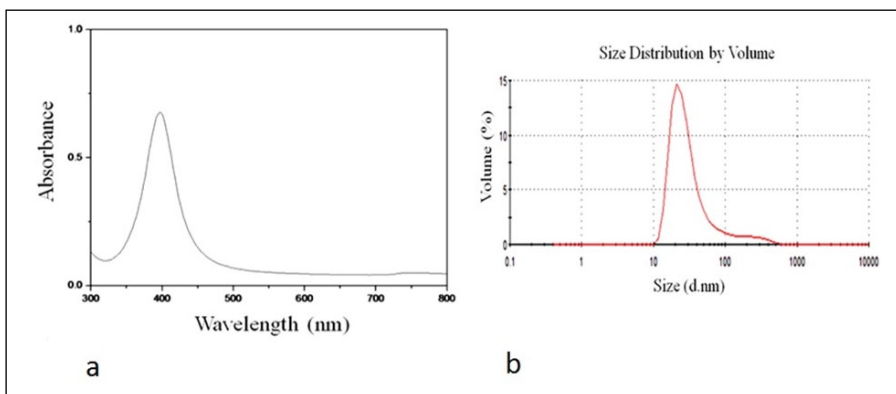
Figure 1. General structure of chitosan.

Figure 2. (a) UV–vis spectroscopy of AgNPs-chitosan and (b) particle size distribution of AgNPs-chitosan obtained by DLS.

Statistical analysis. All the experimental protocols were performed in triplicate and in three independent experiments. Differences between groups were analyzed by one-way analysis of variance (ANOVA) followed by Bonferroni's post hoc test using GraphPad Prism® software version 5.0, considering the differences were statistically significant when $p<0.05$. The IC_{50} and CC_{50} values were calculated using probit analysis (SPSS program, version 20.0) with a confidence level of 95% ($p<0.05$).

Results and discussion

Characterization of silver nanoparticles

Chitosan is a polysaccharide obtained by partial deacetylation of chitin (Figure 1). The chitosan in solution is protonated and positively charged and is able to be adsorbed onto the surfaces of metal nanoparticles, stabilizing and protecting the nanoparticles.

Silver nanoparticles were obtained using chitosan as stabilizing agent. The formation of AgNPs-chitosan was monitored by UV–vis absorption spectra at 300–800 nm, and a plasmon absorption band, characteristic of silver nanoparticles, was observed at 400 nm, as shown in Figure 2(a). The solution at the AgNPs-chitosan resulted in a final Ag^0 concentration of 0.74 mM, as confirmed by the atomic absorption test.

Silver nanoparticles absorb radiation in the visible region of the electromagnetic spectrum (ca. 380–450 nm), due to the excitation of surface plasmon vibrations which is responsible for the striking yellow-brown color (Figure 2(a)) of silver nanoparticles. Figure 1(b) also presents a
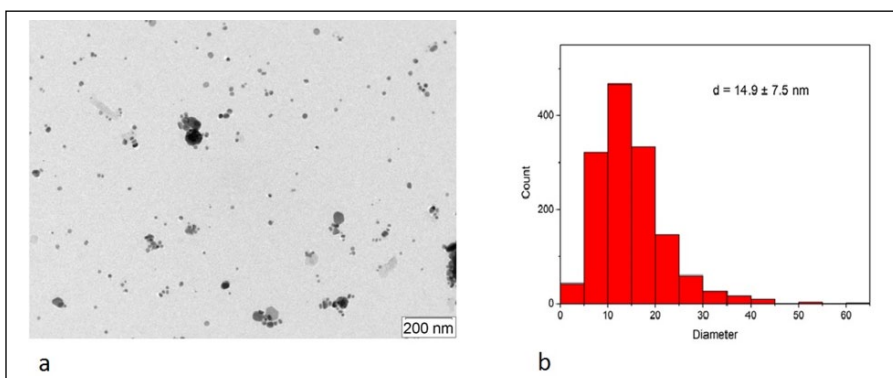
Figure 3. (a) TEM images of AgNPs-chitosan (scale bar = 0.2 μm) and (b) histograms showing the particle size distribution of AgNPs-chitosan by TEM (diameter (d) = 14.9 ± 7.5 nm).
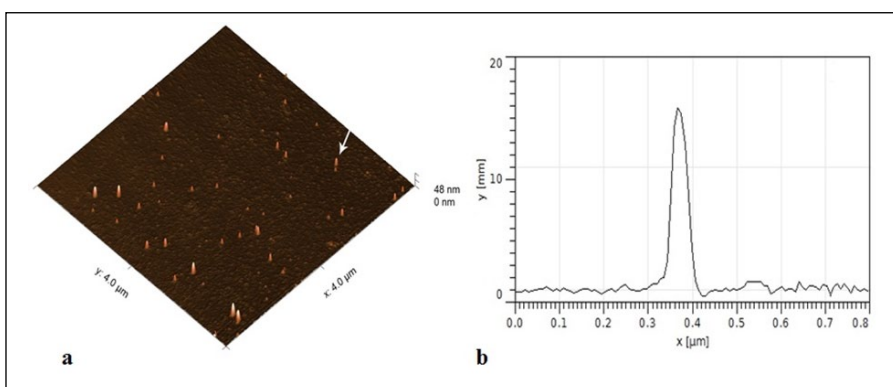

Figure 4. (a) Vibrating mode AFM image of AgNPs-chitosan deposited onto freshly cleaved mica (3D projection of a height image) and (b) profile showing the diameter of a selected particle (arrowed in "a").

particle size distribution obtained from DLS data with the mean particle diameter (d) = 35.6 ± 2.27 nm obtained by DLS.

The average zeta potential (ζ) of the nanoparticles was determined by measuring their electrophoretic mobility, and the values were converted into ζ-potential (mV). The capping of cationic polysaccharide on the surface of nanoparticles was confirmed by zeta potential measurement (+55.0 mV) and is responsible for the electrostatic stability. The average diameters observed by TEM were lower than the corresponding hydrodynamic diameter (36 nm for DLS and 15 nm for TEM; Figure 3(a) and (b)).

These observations are normal and mostly reflect the increased sensitivity of DLS to larger particles, as well as small particle aggregates can be detected in solution, while for TEM only single particles can be counted. On the other hand, the AFM imaging demonstrated a mean diameter of 17.5 nm with a standard deviation of 3.35 nm (Figures 4(a) and (b)). This result is in accordance with TEM results. Unlike TEM, AFM is equally sensitive to soft organic materials, such as chitosan and metallic particles. Therefore, the polymeric coating of the nanoparticles does not increase significantly their size.
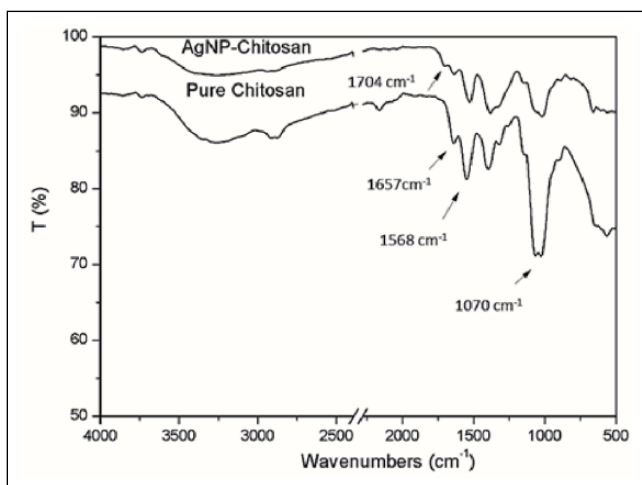
Figure 5. ATR–FTIR spectra of AgNPs-chitosan synthesized with 0.5 M AgNO$_3$ and pure chitosan.

Figure 5 illustrates FTIR spectra of chitosan and AgNPs-chitosan materials synthesized with 0.5 M AgNO$_3$. The broad absorption peak at 4000–500 cm^{-1} is the merged characteristic bands for OH. The NH$_2$ groups[21] and CONH$_2$ absorption band are also observed near 1657 cm^{-1} in the FTIR spectrum of chitosan.[22] The shift was observed from 1657 cm^{-1} in the Ag-loaded chitosan spectra. At the same time, the N–H bending vibration bands at about 1568 cm^{-1} were shifted to 1560 cm^{-1} along with a decrease in intensity. This shift may indicate the binding of AgNPs to an N–H bond of chitosan.[10] The presence of the 1704 cm^{-1} signal may indicate that the reduction in the silver ions is coupled to the oxidation of the hydroxyl groups in the chitosan molecule. The bands near 1080–1025 cm^{-1} are attributed to νCO of the ring COH, COC, and CH$_2$OH. The band at 3419 cm^{-1} corresponds to the combined peaks of the NH$_2$ and OH group stretching vibration in chitosan.

Biological assays

The effects of AgNPs-chitosan against resistant bacterial strains, promastigotes forms of *L. amazonensis*, and murine macrophages were evaluated. The concentration of silver nanoparticles and AgNO$_3$ was presented in micrograms silver per milliliter. For the AgNPs-chitosan solution, besides the reduced silver concentration, the respective concentration of chitosan (µg/mL) present in the respective dilution is shown in parentheses, to support the comparison of biological effects among the different agents present.

In Table 1, the AgNPs-chitosan induced a potent effect against all tested microorganisms at MICs ranging between 1.69 (7.81) and 3.38 (15.63) µg Ag/mL. These values are lower than the MICs obtained for chitosan and AgNO$_3$ solutions. This excellent activity seems to be related to a synergistic effect between the AgNPs and chitosan solution used in stabilization.

The antimicrobial property of chitosan and its derivatives have been attracting great attention from researchers, and studies have reported that the chitosan by itself[23] possess activity against filamentous fungi, yeasts, and bacteria, being more active against Gram-positive than Gram-negative bacteria.[24–29] The main suggested mechanism are related to (a) the binding of cationic chitosan to sialic acid in phospholipids, causing a membrane-disrupting effect, and consequently restraining the movement of microbiological substances,[30] and (b) the penetration of oligomeric

Table 1. Minimum inhibitory concentrations (MICs) of AgNPs-chitosan (µg Ag/mL), chitosan (µg/mL), AgNO$_3$ (µg Ag/mL), and standard antibiotics (µg/mL).

Strain	AgNPs-chitosan	Chitosan	AgNO$_3$	Antibiotic
Staphylococcus aureus (MRSA) ATCC 43300	1.69 (7.81)	31.25	13.5	Vancomycin: 1
Escherichia coli ATCC 35218	1.69 (7.81)	15.6	6.75	Meropenen: <0.5
Klebsiella pneumonia ATCC700603	3.38 (15.63)	31.25	6.75	Meropenen: <0.5

AgNPs-chitosan: chitosan-based silver nanoparticles; MRSA: methicillin-resistant *Staphylococcus aureus*.
Obs.: in parentheses; concentration of chitosan (µg/mL) present in respective AgNPs-chitosan dilution.

chitosan into the cells, where they interact with cellular DNA of fungi and bacteria, consequently inhibiting DNA transcription, as well as RNA and protein synthesis.[31–34]

Several studies have reported that AgNPs induced strong antimicrobial activity against the most microorganisms, including bacteria, fungi, and viruses. In their review article, Prabhu and Poulose[35] reported there are various theories regarding the mechanisms of action of silver nanoparticle–induced microbicidal effects: (a) the nanoparticles can be fixed on the surface and cause the changes in the permeability of the cell membrane and death of the microorganism; (b) the nanoparticles, in contact with the microorganisms, promote the generation of free radicals, then resulting in the formation of pores through the microorganism membrane, loss of osmoregulation, and cell death;[36,37] and (c) the nanoparticle release silver ions[38] which could interact with the thiol groups of many vital enzymes,[39] as well as with sulfur and phosphorus present in DNA and proteins, inactivating these molecules and leading to death of the microorganism. Corroborating our findings, in recent publications, chitin/chitosan/AgNP composites have enhanced antimicrobial activities against microbial pathogens (bacteria, fungi, and virus).[40–42] Comparative studies showed that AgNPs–chitosan composite is much more effective against bacteria than pure chitosan.[10,41,42] Furthermore, Kumar-Krishnan et al.[43] related that synergistic effect of AgNPs and Ag$^+$ ions improving antibacterial effect as well as chitosan help stabilize the AgNPs and prevent AgNPs' agglomeration, also conferring positive charges to nanoparticles' surface, enhancing their binding to the negative charges present in the bacterial cell wall.

The antileishmanial activity of the AgNPs-chitosan, chitosan, and AgNO$_3$ (Figure 6) against promastigote forms of *L. amazonensis* was assessed by resazurin assay. The AgNO$_3$ induced a concentration-dependent anti-*Leishmania* activity, sacrificing more than 50% of the promastigotes exposed at concentrations from 1.69 µg/mL (Figure 6(a)). Chitosan presented leishmanicidal activity at concentrations from 7.81 µg/mL, sacrificing more than 50% of promastigotes at concentrations of 15.63 µg/mL (Figure 6(b)). Interestingly, this activity was lower than the AgNPs-chitosan-induced leishmanicidal activity (Figure 6(c)), where concentrations from 0.84 (3.91) µg/mL sacrificed more than 50% of the promastigotes. As shown in Figure 3, AgNO$_3$, chitosan, and AgNPs-chitosan promoted concentration-dependent anti-*Leishmania* activity. Overall, the effect of chitosan-capped nanoparticles against *Leishmania* was slightly stronger than the same concentration of chitosan alone.

Studies conducted by Said et al.[44] revealed a decrease by 90.6% of the number of *Giardia lamblia* cysts in infected mice and treated with silver nanoparticles and chitosan. However, there is a lack of information about antileishmanial activity of silver nanoparticles alone or together with chitosan.[45,46] Allahverdiyev et al.[45] determined antileishmanial effects of AgNPs on *Leishmania tropica* by examining their effects on various cellular parameters of promastigote and amastigote forms. They used a concentration of 200 µg/mL of AgNPs and demonstrated the most significant antileishmanial effects occurred by inhibiting the proliferation and metabolic activity of promastigotes and inhibited the survival of amastigotes in host cells.
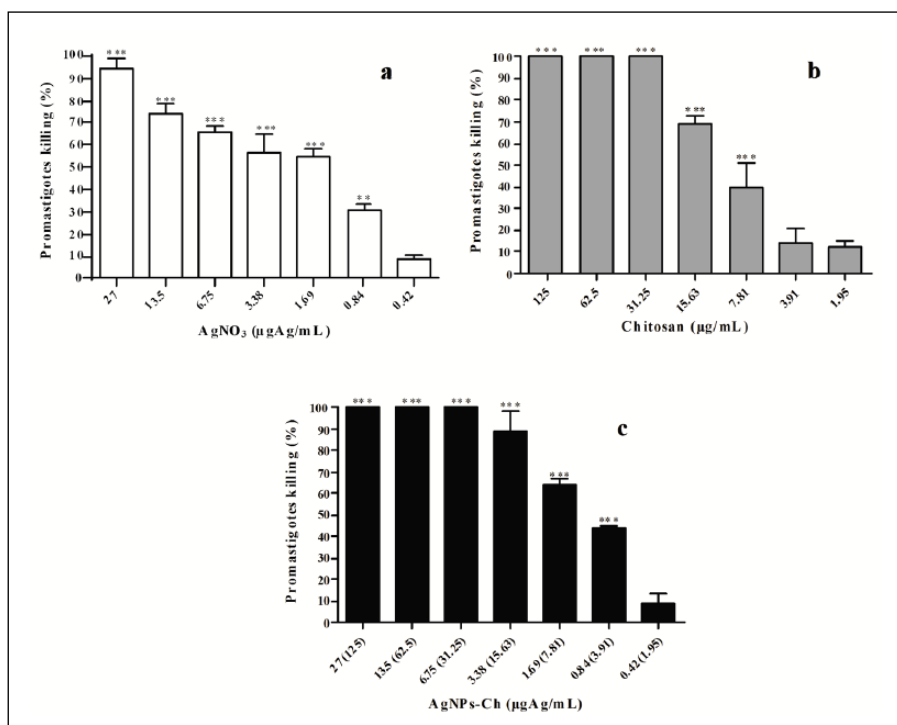
Figure 6. Anti-*Leishmania* activity of the (a) AgNO₃, (b) chitosan, and (c) AgNPs-chitosan against promastigote forms of *L. amazonensis*. Parasites (1×10^6) were exposed to different concentrations for 48 h, and cell viability was assessed by resazurin (alamarBlue®).
***$p < 0.001$ vs control; *$p < 0.05$ vs control; **$p < 0.01$ vs control.

Furthermore, Ribeiro et al.[47] developed a nanoparticle system containing chitosan, chondroitin sulfate, and amphotericin B and then evaluated its antileishmanial activity against in vitro promastigote and in vivo amastigote forms of *L. amazonensis* and *Leishmania infantum*, to develop a less toxic amphotericin B delivery system. In this report, cells infected with *L. amazonensis* and later treated with chitosan and chitosan-based nanoparticles induced a significant reduction in parasite numbers by 24% and 55%, respectively. These findings are consistent with our results showing activity against *Leishmania* at concentrations of 31.25 µg/mL chitosan and 6.75 (31.25) µg/mL chitosan nanoparticles leading to death of 100% of the parasites.

Figure 3 shows the cytotoxic effects of the (a) AgNO₃, (b) chitosan, and (c) AgNPs-chitosan against murine macrophages as a model for mammalian cells. The cytotoxic effects of exposure to ionic silver diminished the MTT reduction capacity of the macrophages, with 80% reduction in activity seen in silver concentrations from 1.69 µg/mL (Figure 7(a)). The chitosan showed cytotoxic effect at concentrations from 15.63 µg/mL (concentrations able to sacrifice 100% of *Leishmania* promastigotes). However, the concentrations from 7.81 µg/mL, which was able to sacrifice 40% of *Leishmania* promastigotes (Figure 7(b)), did not show cytotoxicity against murine macrophages (Figure 7(b)). Moreover, the AgNPs-chitosan showed cytotoxic effect at all tested concentrations. However (Figure 4(c)), there was a significant decrease in this effect with a decrease in concentration, reaching 80% viability of macrophages at concentrations of 0.84 (3.91) µg/mL, corresponding to the concentration able to sacrifice 46% of the promastigotes
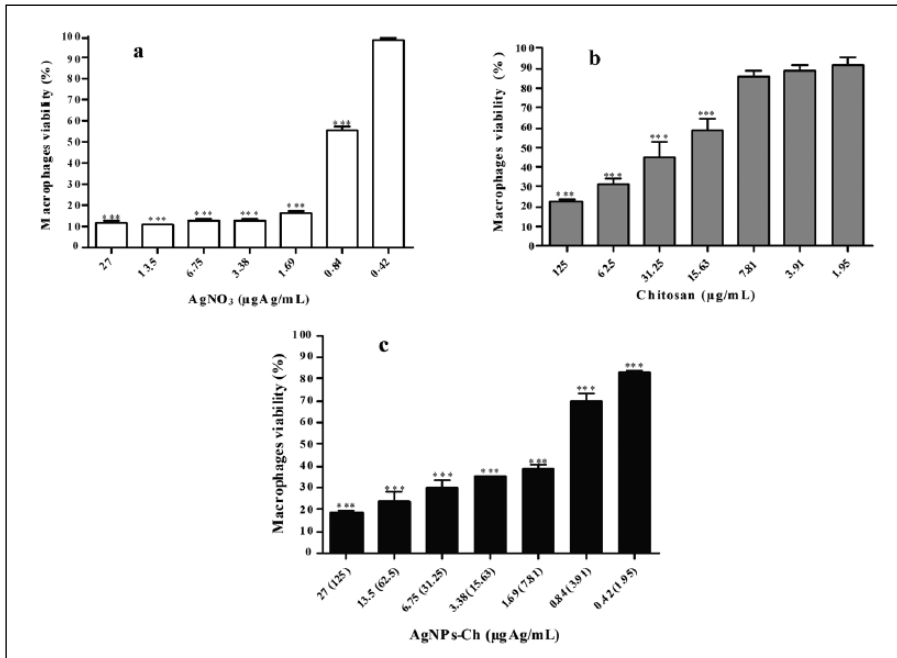
Figure 7. Cytotoxic effects of the (a) AgNO₃, (b) chitosan, and (c) AgNPs-chitosan against murine macrophages. Murine macrophages were incubated for 48 h in the presence of different concentrations. Macrophages' viability was measured by MTT assay. Data are expressed as mean ± SEM of three experiments performed in triplicate.

(Figure 3(c)). Overall, chitosan was found to be considerably less cytotoxic than the AgNO₃, and chitosan–AgNPs demonstrated intermediate toxicity.

Several studies in the literature have demonstrated that ionic silver and AgNPs possess both antimicrobial and anti-inflammatory activities,[48–51] with a marked potential for application in the treatment of various related diseases.[35] However, the cytotoxic effect of nanoparticles is still controversial. Some studies have reported mild or no cytotoxic effect, and other studies have conversely reported moderate to high cytotoxic effects against mammalian cells. Ribeiro et al.[47] have previously demonstrated that chitosan and chitosan-based nanoparticles showed no significant cytotoxicity against mammalian cells at the highest concentration of 100 μg/mL. Interestingly, the percentages of infected macrophages were 66% and 39% after treatment with chitosan and AgNPs-chitosan, respectively. Otherwise, Jebali and Kazemi[46] reported that the nanoparticles promote high cytotoxicity against macrophages, despite its potential antileishmanial activity. On the other hand, some studies have shown that the cytotoxic effect of a compound evaluated by in vitro assays is not always observed in in vivo studies, where the toxicological effects could be influenced by the administration route, among other differences. Furthermore, in their previous studies, Ong et al.[52] have demonstrated that while AgNP-containing chitosan-based wound dressings promote in vitro cytotoxicity, they satisfactorily perform in vivo wound healing effect.

Table 2 summarizes the results of the anti-*Leishmania* activity against promastigote forms of *L. amazonensis*, cytotoxic effects against mammalian cells, and SI values calculated for chitosan, AgNPs, and AgNPs-chitosan. Based on the IC₅₀ against promastigotes, chitosan induced a

Table 2. Antileishmanial and cytotoxic effects of chitosan and AgNPs-chitosan.

Compounds		Promastigotes	Macrophages	SI
		IC_{50} (µg/mL)	CC_{50} (µg/mL)	
Chitosan		2.120 ± 0.238	29.299 ± 8.156	13.82
AgNPs-chitosan	AgNPs	0.422 ± 0.046	2.042 ± 0.632	4.84
	Chitosan	1.959 ± 0.211	9.451 ± 2.928	4.82
AgNPs-chitosan		2.381 ± 0.257	11.493 ± 2.928	9.66
$AgNO_3$		2.584 ± 0.719	0.742 ± 0.545	0.29

SI (selectivity index) = CC_{50}/IC_{50}; AgNPs-chitosan: chitosan-based silver nanoparticles.

Table 3. Mean numbers of amastigote/macrophage at 24 and 48 h after treatment with different concentrations of AgNPs-chitosan and controls.

AgNPs-chitosan concentrations (µg Ag/mL)	Mean number of amastigote/macrophage	
	24 h	48 h
0	4.5 ± 0.6	4.8 ± 0.2
0.42	4.2 ± 0.1	3.5 ± 0.2
0.84	4.0 ± 0.3	3.4 ± 0.2
1.69	3.8 ± 0.2	3.6 ± 0.1
3.38	3.0 ± 0.1	2.7 ± 0.2
6.75	2.3 ± 0.2	2.0 ± 0.1
13.5	1.1 ± 0.1	0.9 ± 0.2
27.0	0.95 ± 0.2	0.8 ± 0.3

AgNPs-chitosan: chitosan-based silver nanoparticles.

leishmanicidal effect similar to the AgNPs-chitosan IC_{50}. However, chitosan was less cytotoxic against macrophages when compared with the AgNPs-chitosan. Interestingly, the high cytotoxicity promoted by $AgNO_3$ is markedly decreased when the silver is nanostructured with chitosan. Besides, the evaluation of the cytotoxic effect of AgNPs against promastigotes and macrophages demonstrates that the AgNPs showed a higher cytotoxic effect than the chitosan either alone or as a part of the nanoparticles' composition.

The intracellular amastigote forms are the life stage responsible for clinical manifestations of leishmaniasis, occurring as an intracellular amastigote in the mammalian host and as promastigotes only in the intestine of the sand fly vector.[53] Therefore, considering the anti-*Leishmania* potential of AgNPs-chitosan, its effects against macrophage-internalized amastigote forms of *L. amazonensis* was evaluated. The AgNPs-chitosan was able to promote a marked decrease in internalized amastigotes in infected macrophages (Table 3). Besides, $AgNO_3$ (27 µg/mL) and chitosan (125 µg/mL) had no activity until the maximum concentration tested in parentheses.

Conclusion

AgNPs-chitosan were synthesized and characterized in this work and presented a marked effect against resistant Gram-positive and Gram-negative pathogenic bacteria. Likewise, AgNPs-chitosan presented less cytotoxicity than silver alone and was more active against *L. amazonensis*

than chitosan alone. Thus, these results demonstrate that the AgNPs-chitosan represent a promising alternative for the treatment of microbial infections and leishmaniasis.

Declaration of conflicting interests

Funding

References

1. Ravi Kumar MN. A review of chitin and chitosan applications. *React Funct Polym* 2000; 46: 1–27.
2. Illum L. Chitosan and its use as a pharmaceutical excipient. *Pharm Res* 1998; 15: 1326–1331.
3. Stulzer HK, Lacerda L, Tagliari MP, et al. Synthesis and characterization of cross-linked malonylchitosan microspheres for controlled release of acyclovir. *Carbohyd Polym* 2008; 73: 490–497.
4. Alves NM and Mano JF. Chitosan derivatives obtained by chemical modifications for biomedical and environmental applications. *Int J Biol Macromol* 2008; 43: 401–414.
5. Bhattacharya R and Mukerjee P. Biological properties of "naked" metal nanoparticles. *Adv Drug Deliv Rev* 2008; 60: 1289–1306.
6. Choi S-J, Oh J-M and Choy J-H. Toxicological effects of inorganic nanoparticles on human lung cancer A549 cells. *J Inorg Biochem* 2009; 103: 463–471.
7. Durán N, Durán M, de Jesus MB, et al. Silver nanoparticles: a new view on mechanistic aspects on antimicrobial activity. *Nanomedicine* 2016; 12: 789–799.
8. Bashiri R, Akhbari K and Morsali A. Nanopowders of 3D Ag^I coordination polymer: a new precursor for preparation of silver nanoparticles. *Inorganica Chim Acta* 2009; 362: 1035–1041.
9. Qadan M and Cheadle WG. Common microbial pathogens in surgical practice. *Surg Clin North Am* 2009; 89: 295–310.
10. Wei D, Sun W, Qian W, et al. The synthesis of chitosan-based silver nanoparticles and their antibacterial activity. *Carbohyd Res* 2009; 344: 2375–2382.
11. Venkatesham M, Ayodhya D, Madhusudhan A, et al. A novel green one-step synthesis of silver nanoparticles using chitosan: catalytic activity and antimicrobial studies. *Appl Nanosci* 2014; 4: 113–119.
12. Khameneh B, Diab R, Ghazvini K, et al. Breakthroughs in bacterial resistance mechanisms and the potential ways to combat them. *Microb Pathog* 2016; 95: 32–42.
13. Nadhman A, Nazir S, Khan MI, et al. PEGylated silver doped zinc oxide nanoparticles as novel photosensitizers for photodynamic therapy against *Leishmania. Free Radic Biol Med* 2014; 77: 230–238.
14. Abamor ES and Allahverdiyev AM. A nanotechnology based new approach for chemotherapy of Cutaneous Leishmaniasis: TIO2@AG nanoparticles—*Nigella sativa* oil combinations. *Exp Parasitol* 2016; 166: 150–163.
15. Sundar S, Singh A and Singh OP. Strategies to overcome antileishmanial drugs unresponsiveness. *J Trop Med* 2014; 2014: 646932.
16. Quelemes PV, Araruna FB, de Faria BEF, et al. Development and antibacterial activity of

cashew gum-based silver nanoparticles. *Int J Mol Sci* 2013; 14: 4969–4981.

17. Carneiro SMP, Carvalho FAA, Santana LCLR, et al. The cytotoxic and antileishmanial activity of extracts and fractions of leaves and fruits of *Azadirachta indica* (A Juss.). *Biol Res* 2012; 45: 111–116.

18. O'Brien J, Wilson I, Orton T, et al. Investigation of the Alamar Blue (resazurin) fluorescent dye for the assessment of mammalian cell cytotoxicity. *Eur J Biochem* 2000; 267: 5421–5426.

19. Rolón M, Vega C, Escario JA, et al. Development of resazurin microtiter assay for drug sensibility testing of *Trypanosoma cruzi* epimastigotes. *Parasitol Res* 2006; 99: 103–107.

20. Esmaeili J, Mohebali M, Edrissian GH, et al. Evaluation of miltefosine against *Leishmania major* (MRHO/IR/75/ER): in vitro and in vivo studies. *Acta Med Iran* 2008; 46: 191–196.

21. Qi L, Xu Z, Jiang X, et al. Preparation and antibacterial activity of chitosan nanoparticles. *Carbohydr Res* 2004; 339: 2693–2700.

22. Murugadoss A and Chattopadhyay A. A "green" chitosan-silver nanoparticle composite as a heterogeneous as well as micro-heterogeneous catalyst. *Nanotechnology* 2008; 19: 015603.

23. Pavinatto FJ, Pavinatto A, Caseli L, et al. Interaction of chitosan with cell membrane models at the air-water interface. *Biomacromolecules* 2007; 8: 1633–1640.

24. Hafdani FN and Sadeghinia N. A review on application of chitosan as a natural antimicrobial. *Int J Med Heal Biomed Bioeng Pharm Eng* 2011; 5: 46–50.

25. Muzzarelli R, Tarsi R, Filippini O, et al. Antimicrobial properties of N-carboxybutyl chitosan. *Antimicrob Agents Chemother* 1990; 34: 2019–2023.

26. Rhoades J and Roller S. Antimicrobial actions of degraded and native chitosan against spoilage organisms in laboratory media and foods. *Appl Environ Microbiol* 2000; 66: 80–86.

27. Jeon Y-J, Park P-J and Kim S-K. Antimicrobial effect of chitooligosaccharides produced by bioreactor. *Carbohydr Polym* 2001; 44: 71–76.

28. Raafat D and Sahl H-G. Chitosan and its antimicrobial potential—a critical literature survey. *Microb Biotechnol* 2009; 2: 186–201.

29. No HK, Young Park N, Ho Lee S, et al. Antibacterial activity of chitosans and chitosan oligomers with different molecular weights. *Int J Food Microbiol* 2002; 74: 65–72.

30. Sashiwa H and Aiba S. Chemically modified chitin and chitosan as biomaterials. *Prog Polym Sci* 2004; 29: 887–908.

31. Tarsi R, Muzzarelli RAA, Guzman CA, et al. Inhibition of *Streptococcus mutans* adsorption to hydroxyapatite by low-molecular-weight chitosans. *J Dent Res* 1997; 76: 665–672.

32. Liu XF, Guan YL, Yang DZ, et al. Antibacterial action of chitosan and carboxymethylated chitosan. *J Appl Polym Sci* 2001; 79: 1324–1335.

33. Rabea EI, Badawy ME-T, Stevens CV, et al. Chitosan as antimicrobial agent: applications and mode of action. *Biomacromolecules* 2003; 4: 1457–1465.

34. Je J-Y and Kim S-K. Chitosan derivatives killed bacteria by disrupting the outer and inner membrane. *J Agric Food Chem* 2006; 54: 6629–6633.

35. Prabhu S and Poulose EK. Silver nanoparticles: mechanism of antimicrobial action, synthesis, medical applications, and toxicity effects. *Int Nano Lett* 2012; 2: 32.

36. Danilczuk M, Lund A, Sadlo J, et al. Conduction electron spin resonance of small silver particles. *Spectrochim Acta A Mol Biomol Spectrosc* 2006; 63: 189–191.

37. Kim JS, Kuk E, Yu KN, et al. Antimicrobial effects of silver nanoparticles. *Nanomedicine* 2007; 3: 95–101.

38. Feng QL, Wu J, Chen GQ, et al. A mechanistic study of the antibacterial effect of silver ions on *Escherichia coli* and *Staphylococcus aureus*. *J Biomed Mater Res* 2000; 52: 662–668.

39. Matsumura Y, Yoshikata K, Kunisaki S, et al. Mode of bactericidal action of silver zeolite and its comparison with that of silver nitrate. *Appl Environ Microbiol* 2003; 69: 4278–4281.

40. Mori Y, Ono T, Miyahira Y, et al. Antiviral activity of silver nanoparticle/chitosan composites against H1N1 influenza A virus. *Nanoscale Res Lett* 2013; 8: 93.

41. Nguyen VQ, Ishihara M, Mori Y, et al. Preparation of size-controlled silver nanoparticles and chitin-based composites and their antimicrobial activities. *J Nanomater* 2013; 2013: 693486.

42. Nguyen VQ, Ishihara M, Mori Y, et al. Preparation of size-controlled silver nanoparticles and chitosan-based composites and their anti-microbial activities. *Biomed Mater Eng* 2013; 23: 473–483.

43. Kumar-Krishnan S, Prokhorov E, Hernández-Iturriaga M, et al. Chitosan/silver nanocomposites: synergistic antibacterial action of silver nanoparticles and silver ions. *Eur Polym J* 2015; 67: 242–251.

44. Said DE, Elsamad LM and Gohar YM. Validity of silver, chitosan, and curcumin nanoparticles as anti-Giardia agents. *Parasitol Res* 2012; 111: 545–554.

45. Allahverdiyev A, Abamor EŞ, Bagirova M, et al. Antileishmanial effect of silver nanoparticles and their enhanced antiparasitic activity under ultraviolet light. *Int J Nanomedicine* 2011; 6: 2705–2714.

46. Jebali A and Kazemi B. Nano-based antileishmanial agents: a toxicological study on nanoparticles for future treatment of cutaneous leishmaniasis. *Toxicol in Vitro* 2013; 27: 1896–1904.

47. Ribeiro TG, Franca JR, Fuscaldi LL, et al. An optimized nanoparticle delivery system based on chitosan and chondroitin sulfate molecules reduces the toxicity of amphotericin B and is effective in treating tegumentary leishmaniasis. *Int J Nanomedicine* 2014; 9: 5341–5353.

48. Ali SW, Rajendran S and Joshi M. Synthesis and characterization of chitosan and silver loaded chitosan nanoparticles for bioactive polyester. *Carbohydr Polym* 2011; 83: 438–446.

49. Wong KKY, Cheung SOF, Huang L, et al. Further evidence of the anti-inflammatory effects of silver nanoparticles. *ChemMed Chem* 2009; 4: 1129–1135.

50. David L, Moldovan B, Vulcu A, et al. Green synthesis, characterization and anti-inflammatory activity of silver nanoparticles using European black elderberry fruits extract. *Colloids Surf B Biointerfaces* 2014; 122: 767–777.

51. Franci G, Falanga A, Galdiero S, et al. Silver nanoparticles as potential antibacterial agents. *Molecules* 2015; 20: 8856–8874.

52. Ong SY, Wu J, Moochhala SM, et al. Development of a chitosan-based wound dressing with improved hemostatic and antimicrobial properties. *Biomaterials* 2008; 29: 4323–4332.

53. Zeledón RA. Hemoflagellates. In: Baron S (ed.) *Medical microbiology*. University of Texas Medical Branch at Galveston, http://www.ncbi.nlm.nih.gov/pubmed/21413333 (1996, accessed 13 September 2016).